*Proc. Natl. Acad. Sci. USA*
Vol. 94, pp. 12198–12203, October 1997
Neurobiology

# Recurrent excitatory postsynaptic potentials induced by synchronized fast cortical oscillations

**(neuronal network/40 Hz/synaptic potentiation)**

MILES A. WHITTINGTON*†, ROGER D. TRAUB‡§¶, HOWARD J. FAULKNER*, IAN M. STANFORD‖, AND JOHN G. R. JEFFERYS‖

*Department of Physiology and Biophysics, Imperial College School of Medicine at St. Mary's, London W2 1PG, United Kingdom; ‡IBM Research Division, T. J. Watson Research Center, Yorktown Heights, NY 10598; §Department of Neurology, Columbia University, New York, NY 10032; and ‖Department of Physiology, The Medical School, University of Birmingham, Birmingham B15 2TT, United Kingdom

*Communicated by Nancy J. Kopell, Boston University, Boston, MA, August 27, 1997 (received for review April 25, 1997)*

**ABSTRACT** **Gamma frequency (about 20–70 Hz) oscillations occur during novel sensory stimulation, with tight synchrony over distances of at least 7 mm. Synchronization in the visual system has been proposed to reflect coactivation of different parts of the visual field by a single spatially extended object. We have shown that intracortical mechanisms, including spike doublet firing by interneurons, can account for tight long-range synchrony. Here we show that synchronous gamma oscillations in two sites also can cause long-lasting (>1 hr) potentiation of recurrent excitatory synapses. Synchronous oscillations lasting >400 ms in hippocampal area CA1 are associated with an increase in both excitatory postsynaptic potential (EPSP) amplitude and action potential afterhyperpolarization size. The resulting EPSPs stabilize and synchronize a prolonged beta frequency (about 10–25 Hz) oscillation. The changes in EPSP size are not expressed during non-oscillatory behavior but reappear during subsequent gamma-oscillatory events. We propose that oscillation-induced EPSPs serve as a substrate for memory, whose expression either enhances or blocks synchronization of spatially separated sites. This phenomenon thus provides a dynamical mechanism for storage and retrieval of stimulus-specific neuronal assemblies.**

Fast gamma-frequency oscillations in discrete neuronal populations have been linked to aspects of higher cognitive function, in particular, the selection and "binding" together of pertinent aspects of a sensory stimulus into a perceived whole (1, 2). The evidence for this link stems from the observation of these oscillations in cortical regions and cell populations devoted to the processing of sensory information of different modalities (3–5) and their ability to provide a framework for controlling temporal interactions between spatially discrete areas (6, 7). What still remains to be elucidated is whether this correlate of novel sensory processing is in any way linked to subsequent memory formation.

The rat CA1 hippocampal region *in vitro* has proven useful for studying the cellular mechanisms underlying synchronized gamma-frequency oscillations. It possesses numerous synaptically interconnected inhibitory interneurons (8), which oscillate as a population at gamma frequencies on tonic excitation (9). It also has well developed recurrent inhibitory connections that allow excitatory pyramidal cells both to influence the firing of interneuron networks and to be influenced by these same inhibitory networks (Fig. 1*A*). In addition, a small number of recurrent excitatory connections from pyramidal cell to pyramidal cell occur (10). Most conventional models of memory formation involve the selective long-term enhancement of excitatory synaptic activity (11) to provide a favored pattern of neuronal intercommunication on representation of the original stimulus (12). Were pyramidal cell to pyramidal cell connections to be selectively inducible in CA1, not only would this suggest a possible memory mechanism, perhaps relevant to perception, but that the phenomenon would be relevant to principal cell communication in the neocortex, wherein recurrent excitatory connections are more frequent (13).

Without recurrent excitatory connections, gamma-frequency oscillations arise in the CA1 region (9, 14) when populations of interneurons, or interneurons and pyramidal cells together, receive slow depolarizing stimuli, as induced by application of agonists of metabotropic glutamate receptors, or by extracellular tetanic stimuli at either one or two sites (15). Interneuron populations alone produce oscillations gated by their mutually induced γ-aminobutyric acid type A ($GABA_A$) inhibitory postsynaptic potentials (IPSPs); such oscillations can be synchronized locally, but on a spatial scale of >1.2 mm long-range synchrony does not occur. However, when pyramidal cells also participate in this oscillation, tight synchrony on spatial scales of at least 3–4 mm can occur. In other words, oscillations generated by interconnected interneurons can be shaped by synaptic interactions between these inhibitory neurons and excitatory pyramidal cells in such a way as to facilitate long-range synchronous firing patterns (16). These synchronizing properties of area CA1 all were predicted by a network model with the following critical structural features: (*a*) synaptic interactions include fast excitatory connections to interneurons, and fast inhibitory connections both between interneurons and from interneurons to pyramidal cells; (*b*) fast inhibitory ($GABA_A$ IPSC) relaxation time constant about 10 ms; (*c*) interneuron–interneuron inhibitory conductances large enough for interneuron populations to synchronize locally; (*d*) axon conduction delays between neighboring cell groups of at least 2 ms; (*e*) synaptic excitation of interneurons sufficient for interneuronal spike doublets to occur when pyramidal cells fire synchronously (a critical feature for generating long-range synchrony; ref. 16); and (*f*) driving currents (or conductances) to interneurons narrowly dispersed. Data from the above model predict that long-range synchrony of gamma oscillations can occur without recurrent synaptic connections between pyramidal cells (9, 16).

Using tetanic stimuli above threshold for eliciting these patterns of synchronous oscillations alone, we demonstrate here that the gamma oscillations lead to a stable, synchronous beta-frequency oscillation associated with an increase in recurrent EPSP amplitude.

The publication costs of this article were defrayed in part by page charge payment. This article must therefore be hereby marked "*advertisement*" in accordance with 18 U.S.C. §1734 solely to indicate this fact.



Abbreviations: EPSP, excitatory postsynaptic potential; AHP, afterhyperpolarization; IPSP, inhibitory postsynaptic potential; NBQX, 6-nitro-7-sulfamoylbenzo[*f*]uinoxaline-2,3-dione; RMP, resting membrane potential.

†To whom reprint requests should be addressed. e-mail: m.whittington@sm.ic.ac.uk.
¶Present address: Department of Physiology, The Medical School, University of Birmingham, Birmingham, B15 2TT, U.K.

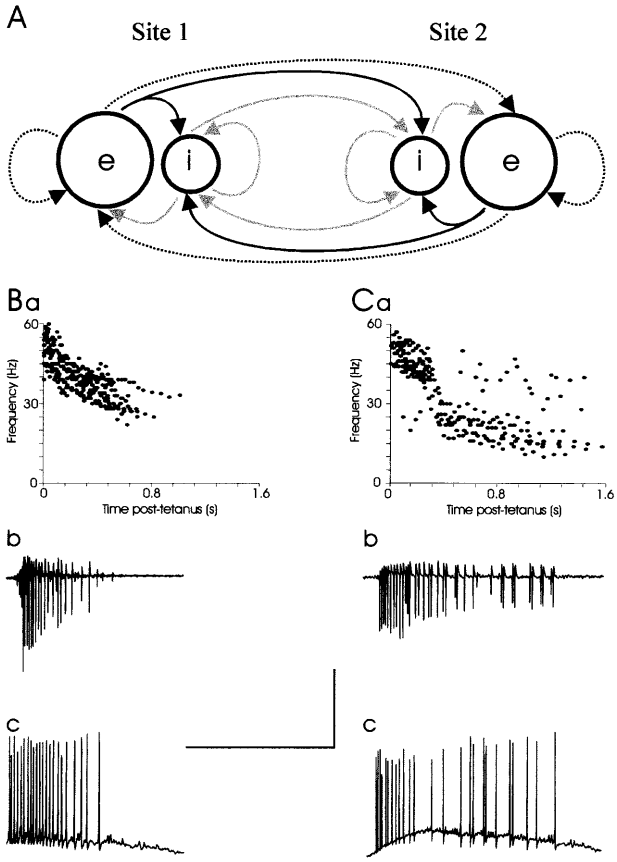


FIG. 1. Supra threshold-paired tetani generate a frequency switch. (*A*) Schematic diagram of the synaptic connections between and within two sites in area CA1 of the hippocampus. e, pyramidal cell population; i, interneuron population. Black lines indicate excitatory connections, gray lines inhibitory connections, and dotted lines recurrent excitation. (*B*) Fast oscillations generated by single-site tetani. (*a*) Plot of instantaneous frequency for 12 trains of population spikes generated by a single-site tetanus at threshold for oscillation. Oscillations lasted 0.3–1.1 s and showed a steady frequency decline before termination. (*b*) Example extracellular recording of population spike oscillations seen after single-site tetanus. Tetanus omitted for clarity. (*c*) Intracellular pyramidal cell recordings reveal no frequency shift. Traces shown begin immediately post-tetanus at pre-tetanus; RMP = −67 mV. (*C*) Fast oscillations generated by two-site tetani at 2× threshold. (*a*) Plot of instantaneous frequency for 10 trains of populations spikes showing initial fast (40–55 Hz) oscillation rapidly switching to slower (10–30 Hz) oscillation and appearance of population spike doublets. (*b*) Example extracellular recording showing prolonged oscillation, frequency switch, and spike doublets (10/10 runs). (*c*) Intracellular recordings showing frequency shift and action potential doublets (RMP = −69 mV). [Scale bar = 1 s, 5 mV (*b*), and 50 mV (*c*).]

## METHODS

Transverse dorsal hippocampal slices were prepared from male Sprague–Dawley rats (200–250 g, $n = 52$) and maintained *in vitro* as described in Traub *et al.* (14). Brief tetanic stimuli (20 pulses, 50 $\mu$s duration, 100 Hz) were applied to one site only or simultaneously applied to two sites. Stimulating electrodes were placed in the stratum oriens proximal to two recording sites at either end of CA1 (CA1a, CA1c, separation 1.5–3 mm). Threshold values for synchronous oscillations were 4–12 V. Four distinct stimulus protocols were used: (*a*) one-site tetanus at threshold for gamma oscillations; (*b*) two-site tetanus at threshold for gamma oscillations; (*c*) one-site tetanus at twice threshold for gamma oscillations; and (*d*) two-site tetanus at twice threshold for gamma oscillations. Extracellular field potentials were recorded simultaneously at both sites at the level of stratum pyramidale using glass microelectrodes filled with 2 M NaCl (1–5 MΩ). Microelectrodes filled with 2 M potassium acetate or methylsulfate (30–65 MΩ) were used for paired intracellular recordings from pyramidal-cells.

The nature of EPSPs seen during beta oscillation was examined using pressure ejection (60 psi, 50–150 ms) of artificial cerebrospinal fluid containing 20 $\mu$M 6-nitro-7-sulfamoylbenzo[*f*]quinoxaline-2,3-dione (NBQX) to block fast ionotropic glutamatergic synaptic activity. The role of postsynaptic action potentials was investigated by recording from pyramidal cells using electrodes filled with 2 M potassium acetate and 50 mM QX314 to block sodium spikes. In one experiment, 200 $\mu$M picrotoxin also was included in the recording electrode to block $\gamma$-aminobutyric acid type A receptor-mediated IPSPs.

The origins and effects of EPSPs on emergent network oscillations was investigated using a computer model. The network structure was that of Traub *et al.* (16): 40 pyramidal cells and 40 inhibitory interneurons, partitioned into five cell groups in a chain (see fig. 1 of ref. 16) with synaptic interactions between pyramidal cells and interneurons, interneurons and interneurons (as above), and now pyramidal cells and pyramidal cells. These connections were present between cells in the same group, and between cells in neighboring groups. Axon conduction delays between groups were 4 ms, and pyramidal cell–pyramidal cell synapses were localized to the basal dendrites (17). $g_{Ca}$ density was decreased (2-fold) and $g_{K(AHP)}$ increased (2.5-fold) to reduce the tendency of the cells to generate intrinsic bursts. The apical dendrites of pyramidal cells received a tonic excitatory conductance of 120–122 nS unless stated otherwise, reversal potential 60 mV positive to resting potential. $\alpha$-amino-3-hydroxy-5-methyl-4-isoxazolepropionic acid receptor-mediated pyramidal cell-pyramidal cell EPSPs were modeled using a 2-ms alpha function and peak conductance of 2.76 nS. Further information on the model is available from R.D.T. (e-mail: r.d.traub@bham.ac.uk).

Auto- and cross-correlation analyses were performed on 200-ms epochs (experiments) and 750 ms (simulations), using Spike2 software for experiments (CED, Cambridge, U.K.). All statistical analyses were performed using two-way ANOVA with multiple comparisons.

## RESULTS

**Threshold Stimuli Evoke Only Gamma-Frequency Oscillations, but Twice-Threshold Stimuli Evoke Gamma Followed by Beta Activity.** A one-site tetanus, at threshold for generating a post-tetanic oscillation, produced a response consisting of a train of population spikes/action potentials at gamma frequency (35–60 Hz), the frequency decreasing over time (Fig. 1*B*). A similar response was elicited by two-site tetanic stimuli at threshold intensity. Stimuli at 2× threshold, delivered to either one or two sites, generated a longer gamma oscillation, which was interrupted after 100–500 ms by a switch in frequency down to 10–30 Hz. This slower beta frequency was stable for >1 s. The beta oscillation contained occasional population spike/action potential doublets (Fig. 1*C*). The slower oscillation was associated with pyramidal cell action potential firing every 2–5 periods of a smaller subthreshold oscillation. The strength of the evoking tetanus, therefore, appeared to alter the temporal pattern of rhythmicity of the induced oscillation, whether one or two sites were stimulated.

**Stimulation at Either One or Two Sites at Twice-Threshold Intensity Leads to Rhythmic Depolarizing Potentials and Enhanced Synchrony During the Latter Part of the Oscillation.** Two-site stimuli at threshold intensity were not sufficient to cause a gamma → beta frequency shift. The post-tetanic oscillation at either site resembled that seen for a single-site tetanus (compare Fig. 1*B* with Fig. 2*A*). The initial gamma-frequency oscillation was highly synchronous between the two sites, but cross-correlation analysis of the end of these oscillations revealed that this synchrony decayed along with the oscillations themselves (Fig. 2*Ab*). Paired intracellular recordings, from pyramidal cells (one at each site), during subsequent oscillations evoked by threshold stimuli,

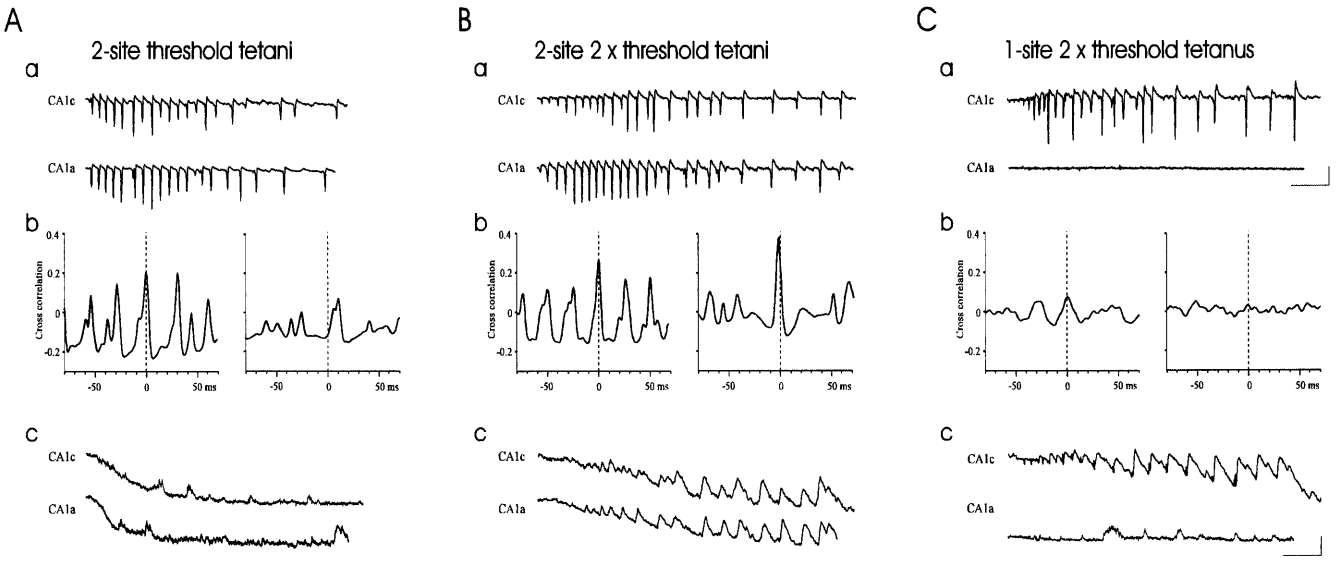


FIG. 2. Synchrony is enhanced after the frequency shift at two sites. (*A*) Control oscillations generated by threshold tetani at two sites. (*a*) Fast population spike oscillations (38 Hz) are generated at both CA3 end (CA1c) and subicular end (CA1a) of area CA1. Oscillations decay after 300 ms and terminate after 1 s. Oscillation traces are shown starting immediately after the end of the tetanus for clarity. (*b*) Initial fast oscillations (first 200 ms post-tetanus) are highly rhythmic and synchronous (*Left*) but decay and become asynchronous during the last 200 ms of the response (*Right*). (*c*) Simultaneous intracellular recordings from two pyramidal cells hyperpolarized to −80 mV (CA1c) and −82 mV (CA1a) with DC current injection. (*B*) Oscillations generated by two-site, 2× threshold tetani are prolonged and show a marked frequency shift. (*a*) Simultaneous extracellular recordings from either end of CA1 show initial fast oscillation (36 Hz) switching to a slower rhythm (c. 15 Hz). (*b*) Initial fast oscillations (first 200 ms) are highly rhythmic and synchronous (*Left*), beta oscillations are less rhythmic but still synchronous (*Right*, overall phase lag was 1.2 ± 0.3 ms, $n = 10$). (*c*) Simultaneous pyramidal cell recordings from hyperpolarized pyramidal cells at both sites for two-site tetani after the initial two-site, 2× threshold tetani. RMPs = −79 and −82 mV. (*C*) (*a*) Oscillations generated by a single-site, 2× threshold tetanus at CA1c showing a gamma/beta frequency shift at the stimulated site only. (*b*) Cross-correlations, as expected, were poor. (*c*) Rhythmic trains of depolarizing potentials were seen at the stimulated site only. RMPs = −86 and −80 mV). (Scale bars = 100 ms, 2 mV.)

showed small depolarizing potentials that were neither rhythmic nor synchronous (Fig. 2*Ac*).

In contrast to two-site stimuli at threshold, two-site stimuli at twice threshold produced an abrupt gamma → beta frequency shift that occurred simultaneously at both sites (Fig. 2*B*). In this case, the synchrony between sites was preserved, or even enhanced, as the oscillations continued at beta frequencies (Fig. 2*Bb*). Both the gamma → beta frequency shift and the preservation of synchrony were associated with a marked enhancement of the depolarizing potentials that were observed when subsequent oscillations were evoked with twice-threshold stimuli (Fig. 2*Bc*). The depolarizing potentials increased in amplitude during the gamma oscillation and persisted throughout the beta oscillation. The depolarizations were rhythmic and synchronized between the two sites. The population spikes in Fig. 2*B* were of comparable size to those in Fig. 2*A*, so that the depolarizing potentials were unlikely to result simply as an accidental byproduct of increased synchrony of action potentials. The gamma → beta shift and the depolarizing potentials were a consequence of stimulus intensity and not of the number of sites stimulated; both the frequency shift and the depolarizing potentials could be generated by a single-site tetanus at twice threshold (Fig. 2*C*). No population activity was seen at the unstimulated site in this case, although small depolarizing potentials are just discernible with intracellular recording during subsequent oscillations (Fig. 2*Cc*).

**A Single Episode of Oscillations Induced by a Twice-Threshold Stimulus Allows Subsequent Threshold Stimuli to Induce Beta and Alters the Synchrony of Subsequent Oscillations Induced by Threshold Stimuli.** Long-term consequences of twice-threshold stimulation were measured in two situations. First, after a period of two-site threshold stimuli (delivered every 4 min for 12–24 min to provide a control period), a single two-site twice-threshold stimulus was delivered (Fig. 3, ●). Subsequent oscillations were elicited using the control (threshold) two-site tetani for 80 min. Analysis of the cross-correlation peak amplitude at 0 ms for the last 200 ms of the oscillation revealed a marked increase in synchrony during the beta-frequency oscillation that now was present. This increase in synchrony remained on returning to control (threshold) stimuli for over 1 hr (Fig. 3*A*). Second, after control (threshold) stimuli as above, a single one-site tetanus at 2× threshold was delivered (Fig. 3, ○). Again, subsequent oscillations were evoked using the threshold two-site tetani for >30 min. In this case, analysis of the cross-correlation peak amplitude at 0 ms for the first 200 ms of the oscillation showed a marked decrease in synchrony for gamma oscillations induced by a single-site, 2× threshold stimulus (Fig. 3*B*). This decrease in gamma synchrony persisted for over 30 min on returning to two-site threshold tetani. In summary, a twice-threshold-induced oscillatory episode induces long-lasting effects on the synchrony of subsequent oscillations; the exact nature of these effects depends on whether the twice-threshold episode was induced at one site or at two sites.

**AHPs Increase During the Course of a Gamma Oscillation.** To investigate the causes of the gamma → beta shift and the oscillation-induced depolarizing potentials, we measured the action potential AHP and depolarizing potential amplitude for each oscillation period, from the start of the post-tetanic oscillation. AHPs were small or absent during the first 4–8 periods (c. 100–200 ms), but recovered rapidly after this (Fig. 4*Aa*). Such an effect was consistent with the activation, by the tetanus, of metabotropic glutamate receptors (18), although some increase in extracellular potassium ion concentration post-tetanus (15) also was found. The pattern of initial absence and recovery of AHPs was present in oscillations after both threshold and 2× threshold paired tetani, i.e., without or with the frequency shift. The size of the AHPs measured immediately preceding the frequency shift was variable (2.7 ± 1.4 mV, $n = 6$).

**Depolarizing Potentials Increase During the Course of an Oscillation, Provided the Stimulus Is Intense Enough to Cause Beta Activity; Depolarizing Potentials Are NBQX-Sensitive and Presumably EPSPs.** Depolarizing potential amplitude showed a pattern of increasing size with each consecutive period of the

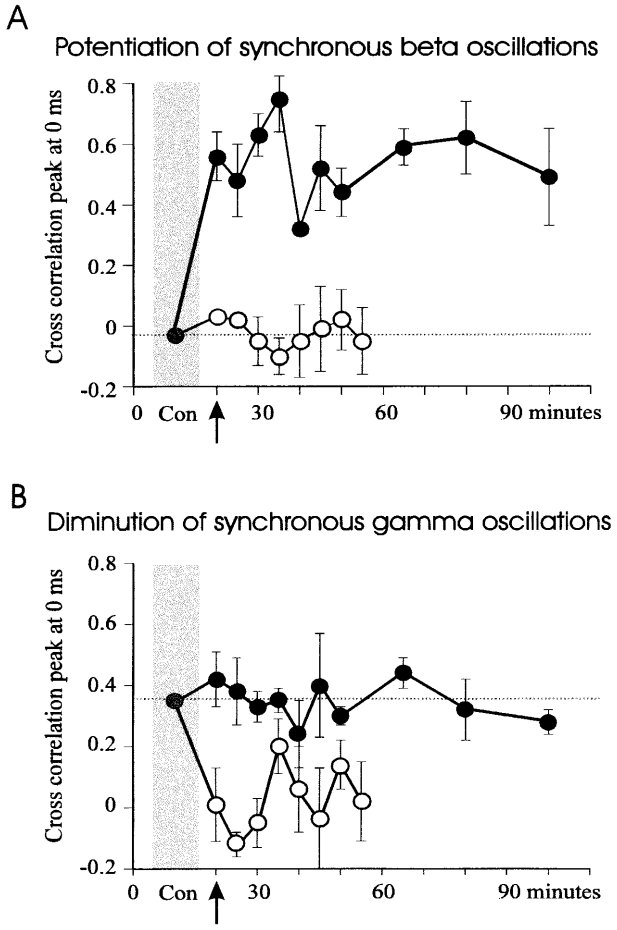


FIG. 3. EPSP induction has long-lasting, site-specific effects on subsequent oscillatory events. All stimuli were two-site, threshold tetani (con) other than indicated by arrows (see below). (*A*) Between-site correlations (at 0 ms) for the last 200 ms of post-tetanic oscillation. A two-site tetanus at 2× threshold (arrow, ●) generated a marked increase in synchrony at beta frequencies, which was maintained for >90 min (●, $n = 4$, $P < 0.01$, two-way ANOVA for the first 30 min). A single-site, 2× threshold tetanus (arrow, ○) produced no effect on the lack of synchrony at the end of the oscillation observed in the control situation (○, $n = 5$). (*B*) Between-site correlations (at 0 ms) for the first 200 ms of post-tetanic oscillation. A single-site, 2× threshold tetanus (arrow, ○) produced a lasting (>30 min) decrease in between-site synchrony or an anticorrelation (○, $n = 5$, $P < 0.05$, two-way ANOVA for the first 30 min). Two-site, 2× threshold tetani (arrow, ●) did not alter synchrony during the gamma oscillation.

oscillation (Fig. 4*Ab*). This was seen only in oscillations with a clear frequency shift. Mean depolarizing potential amplitudes for control oscillations (threshold stimulation) were approximately zero. The depolarizing potential size immediately before the frequency shift was 0.7 ± 0.4 mV ($n = 6$). Depolarizing potentials never reached this mean value in oscillations without a frequency shift, suggesting a relationship between these potentials and the generation of beta oscillations. Addition of pyramidal cell–pyramidal cell excitatory synaptic connections to the computer network model led to beta-frequency oscillations (Fig. 4*B* model). Finally, pressure ejection of the α-amino-3-hydroxy-5-methyl-4-isoxazolepropionic acid receptor blocker NBQX, immediately after the tetanus, abolished or dramatically reduced the depolarizing potential size, and also prevented the frequency shift (8 of 10 slices, Fig. 4*C*). These data suggest that the depolarizing potentials were indeed EPSPs.

**When EPSPs Occur During the Course of an Oscillation, Functional Connectivity Increases Between CA1 Pyramidal Cells and Is Expressed During the Oscillation Itself.** Action

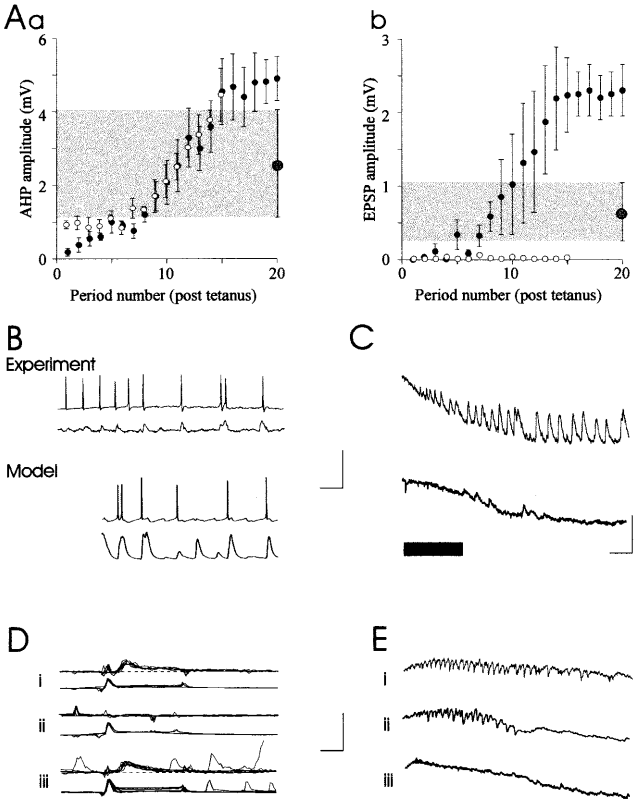


FIG. 4. Stable frequency shifts are caused by EPSP expression. (*A*) (*a*) Post-spike AHP size increases during oscillations either expressing EPSPs (and frequency shift) (●, $n = 6$) or not (○, $n = 5$). Data expressed as mean ± SEM. Shaded area represents AHP size seen immediately pre-frequency switch where present. (*b*) Mean EPSP size increases significantly, 100–400 ms, post-tetanus in runs showing frequency shift (●) but not in runs with no frequency shift (○). Shaded area represents EPSP amplitude immediately pre-frequency shift where present. (*B*) Example of AHP and EPSP amplitude increase associated with frequency shift after two-site tetanus. Two pyramidal cells were impaled in one area (separation c. 80 μm). (*Upper*) A pyramidal cell with RMP = −70 mV. (*Lower*) A neighboring pyramidal cell injected with hyperpolarizing current (RMP = −79 mV). [Scale bar, 100 ms, 50 mV (*Upper*) and 5 mV (*Lower*). Below are two somatic potential traces from the computer model. (*Upper*) Normal RMP. (*Lower*) A different pyramidal cell in the group hyperpolarized with current scaled to −3 nA. [Scale bars, 100 ms, 50 mV (*Upper*) and 10 mV (*Lower*). (*C*) Effects of pressure ejection of NBQX on EPSPs in hyperpolarized cells during oscillations subsequent to initial EPSP potentiation. (*Upper*) Control. (*Lower*) Same cell with NBQX ejected onto stratum oriens (dark bar). RMPs = −86 mV and −85 mV, respectively. (Scale bar = 200 ms, 8 mV.) (*D*) Action potentials generated in a pyramidal cell in site 1 (CA1c, *Lower*) can elicit an EPSP in a pyramidal cell in site 2 (CA1a, *Upper*) during the slower oscillation (*i*) but not afterward (*ii*). However, EPSPs are re-expressed during further tetanically induced oscillations (*iii*). All cells were at normal RMP (−65 to −70 mV). [Scale bar = 10 ms, 0.5 mV (CA1a), 180 mV (CA1c).] (*E*) Post-tetanic response in a cell containing QX314. Strong tetanus generates inhibitory gamma only (*i*). Subsequent control tetani generate few EPSPs (*ii*). Underlying oscillation is absent in cells impaled with QX314 and 200 μM picrotoxin (*iii*). Cells were injected with 0.3 nA depolarizing current to expose underlying IPSPs (RMPs = −55 mV *i* and *ii*, −57 mV *iii*). (Scale bar = 200 ms, 5 mV.)

potentials were generated in a cell at one site by brief depolarizing current pulses (1 nA, 10–20 ms). Pulses were delivered every 200 ms after the initial tetanic stimulus until the next tetanus. No EPSPs were seen in the pyramidal cell simultaneously recorded at the other CA1 site, at any time after the post-tetanic depolarization had ended (in 0 of 15 pairs, Fig. 4*Dii*). During the oscillation itself, however, action potentials in a cell at one site were seen to generate an EPSP

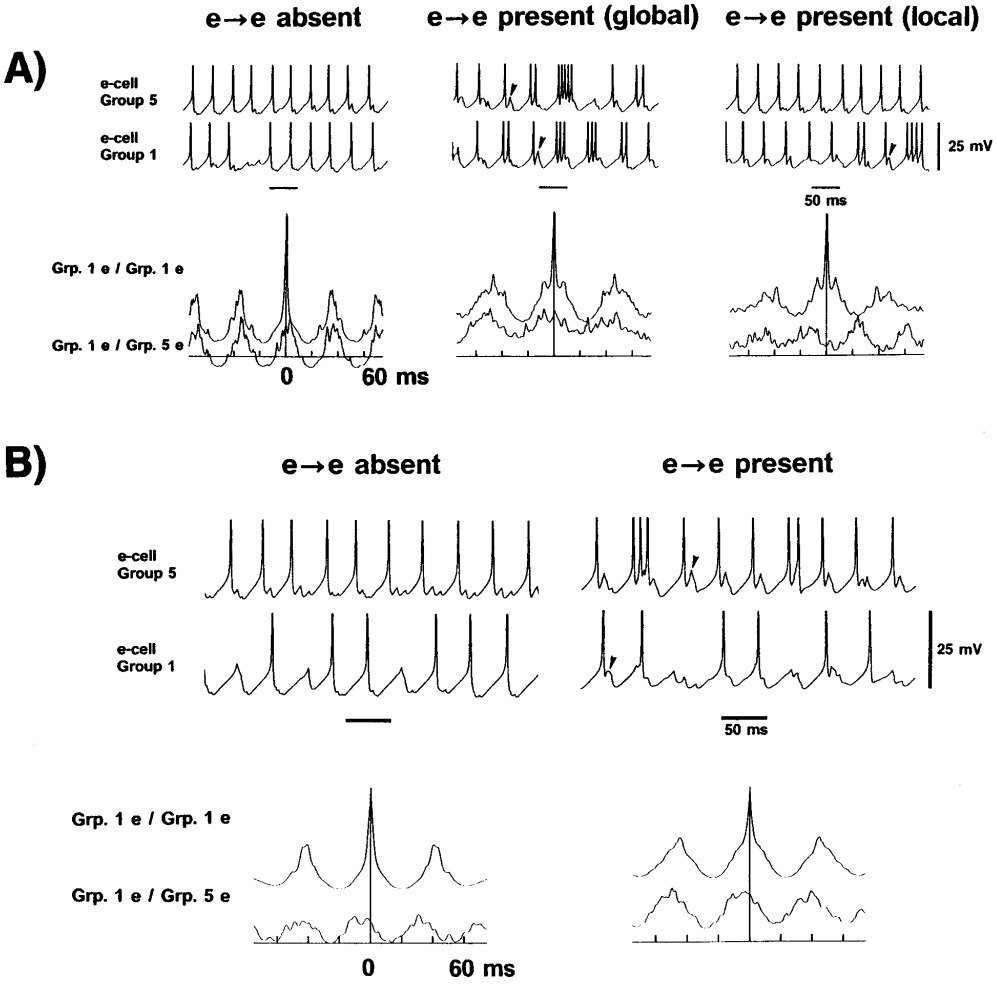


FIG. 5. Site-specificity of recurrent EPSP effects (model). (*A*) In network simulations, recurrent EPSPs, present in only one area, produce asynchrony between gamma oscillations in that area and gamma oscillations in an adjacent area. e-cell (e) denotes pyramidal cell. When recurrent excitation is absent (*Left*), oscillations are tightly synchronized between cell groups 1 and 5 (at opposite ends of the network), owing to the presence of interneuron doublets (not shown). Similarly, when recurrent excitation is present in spatially uniform fashion (*Center*), correlation across the network still exists. EPSPs tend to appear after action potentials (eg. arrowheads). When EPSPs are present only in groups 1 and 2 (*Right*), however, then groups 1 and 5 lose their correlation. (*B*) In simulations, recurrent EPSPs can tighten synchronization between distant oscillating sites when a spatial gradient in pyramidal cell stimuli exists. The tonic excitatory synaptic conductance to pyramidal cell apical dendrites (four compartments) was spatially nonuniform, ranging from 60 nS in group 1 to 120 nS in group 5. Recurrent EPSPs were absent in the left simulation. In the right simulation (eg., arrowhead) they were spatially uniform but the conductance increased with time (as in many of the experiments), unitary peak conductance increasing from 1.97 nS to 2.34 nS over the illustrated interval. Introducing recurrent EPSPs reduces the group 1/group 5 phase lag from 6 ms to 2.5 ms and increases the cross-correlation amplitude by 35%.

in the cell at the other site (2/15 pairs, Fig. 4 *Di* and *Diii*). These EPSPs appeared to be of uniform amplitude (0.4 ± 0.05 mV, 20–40 ms duration) when present, and occasionally elicited an action potential during the post-tetanic depolarization.

**Action Potentials Must Occur in a Pyramidal Cell During the Twice-Threshold-Induced Oscillation for That Cell to Express EPSPs in Subsequent Oscillations.** We recorded from cells in three slices with electrodes filled with the sodium channel blocker QX314 (Fig. 4 *Ei* and *Eii*). This protocol left an underlying inhibitory gamma oscillation intact, i.e., rhythmic IPSPs occurred in the recorded cell. During a two-site, 2× threshold tetanus, no action potentials were seen in these experimental conditions, and only infrequent, aperiodic EPSPs appeared during the now subthreshold oscillation. Further paired tetani at control intensities showed no rhythmic EPSP generation (Fig. 4*Eii*). Consistent with these data, EPSPs were much smaller in pyramidal cells (not illustrated) that were hyperpolarized during the initial two-site, 2× threshold stimulus, as compared with EPSPs in pyramidal cells that were hyperpolarized only during subsequent threshold stimuli, as in Fig. 2*Bc*.

**In Network Simulations, EPSPs Localized to One Part of the Network Interfere with Global Synchrony.** We used network simulations to see if pyramidal cell–pyramidal cell excitation would replicate the above findings. When nearly uniform tonic excitatory conductances were delivered to model pyramidal cell dendrites and excitatory connections were present between pyramidal cells, synchronized gamma oscillations occurred. EPSPs were produced in pyramidal cells (Fig. 4*B* model). Two main patterns emerged in the simulations. First, when driving conductances to the pyramidal cells were nearly uniform (1.7% variation across the array, Fig. 5*A*), with recurrent EPSPs either absent or present in spatially uniform fashion, then synchronized gamma oscillations occurred with near-zero phase lag. In contrast, when recurrent EPSPs were present in spatially localized fashion (cell groups 1 and 2 only, i.e. 40% of the cells), then correlation was lost between oscillations at opposite ends of the network. This detrimental effect on synchrony required the appearance of pyramidal cell spike doublets (and longer multiplets): when EPSPs were too small to induce doublets, the two ends of the array remained in phase to within 3.5 ms. The asynchrony that results from the spike doublets arises in part from a frequency mismatch across the array: in the example of Fig. 5*A* with local recurrent EPSPs, the end of the array without EPSPs oscillates at

28 Hz; whereas the the end with EPSPs exhibits two peaks in its autocorrelation, at 21 Hz and 26 Hz.

**In Simulations EPSPs Throughout the Network Favor Synchrony in the Presence of Nonuniform "Drive."** The second effect in the model appeared when a linear gradient of pyramidal cell driving conductances was used, producing a 2-fold difference in conductance across the array. A 6-ms phase lag was seen between opposite ends of the network without EPSPs (Fig. 5B). When this simulation was repeated with EPSPs present (and spatially uniform), then the phase lag was reduced from 6 ms to 2.5 ms. The reduction in phase lag was caused in part by the tendency of those pyramidal cells receiving the largest driving conductance (group 5) to fire spike multiplets in response to the recurrent EPSPs. These multiplets would tend to reduce the oscillation frequency of the most excited regions, and thereby provide a better frequency match between the ends of the array.

## DISCUSSION

The present observations indicate that synchronous gamma-frequency oscillations in spatially separate areas of hippocampal CA1 can lead to synchronous beta oscillations, associated with the recovery of an AHP and with potentiation of recurrent EPSPs. These phenomena occur together when the gamma oscillations are evoked by stimuli of sufficient intensity. The AHP recovery, during the tail of the post-tetanic depolarization, contributes to the shift in frequency from gamma to beta. EPSPs do not appear necessary for gamma oscillations to occur, but without EPSPs the beta oscillations become asynchronous and break up. A critical feature of this proposed mechanism for beta oscillations is that the EPSP amplitude has to reach a certain value before the AHP recovers. The large number of pyramidal cell–pyramidal cell connections in the neocortex suggests that EPSP amplitude could reach the necessary value more readily in neocortex than in hippocampus. A switch from gamma to beta within 100 ms of presentation of a visual stimulus appears to occur in the human visual cortex (19), and synchronous beta oscillations are seen to develop within 200 ms of presentation of a visual cue, leading to a visuomotor reflex (20).

The absence of functional EPSP potentiation, and of the gamma → beta switch, during oscillations induced by relatively weak stimuli, indicates a mechanism by which the cortex could distinguish between novel, interesting stimuli and unattended stimuli. EPSP potentiation occurs progressively during the gamma oscillation and must reach a threshold value to prevent termination of the rhythm as AHP amplitude increases. Brief oscillations, or oscillations involving too few pyramidal cells, might not cause sufficient EPSP potentiation to maintain rhythmicity and synchrony.

Gamma oscillations at a single site, or synchronous oscillations at two sites, generated rhythmic EPSPs locally or dually, respectively. The marked reduction in EPSP generation when QX314 was injected into an individual neuron suggests a requirement for action potentials in the postsynaptic cell (21). We would expect that such action potentials need to occur with precise timing relative to the EPSPs (22) for potentiation to take place. Dendritic invasion of action potentials occurs in hippocampal neurons (23–25), although it can be blocked by IPSPs (26). The temporal pattern of coincidence between IPSP decay, pyramidal cell firing, and immediately subsequent EPSPs, as occurs during gamma oscillations, suggests a means to orchestrate appropriate timing between cell firing and the arrival of EPSPs. During gamma oscillations, action potentials occur between IPSPs, and so are most likely to invade dendrites. The lack of experimental intervention during the oscillation in our studies, i.e., the fact that temporal patterns of coincidence are generated autonomously by the neuronal network itself, suggest that this mechanism of EPSP potentiation might work *in vivo*, coupling oscillations induced by attention to novel stimuli to alterations in subsequent properties of the network.

Simulations correctly predict that an increase of pyramidal cell AHP, and activation of pyramidal cell–pyramidal cell synapses lead to a decrease in oscillation frequency and to an alteration in between-site synchrony. Local (1-site) EPSP potentiation produces a decrease in between-site synchrony and prevent the formation of coherent temporal relationships during subsequent paired oscillations. Simulations suggest that this is caused by the frequency mismatch between the two sites. However, when EPSPs are of sufficient magnitude throughout the network, synchrony can be enhanced.

In conclusion, *in vitro* hippocampal tissue can develop plastic changes that possibly are caused by neuronal network correlates of cognition. That oscillations could strengthen recurrent excitatory connections was proposed for the olfactory bulb almost 20 years ago (27). The fast oscillations themselves appear to provide both a mechanism for the induction of these plastic changes (28) and a mechanism for "reading" the plastic changes at a later time. In other words, the cellular response to novel stimuli could bring into play a mechanism for memory formation and utilization in the absence of other external influences. Our experimental model provides a direct link between biophysical events at single synapses and observable events taking place in large neuronal populations.

This paper is dedicated to the memory of Dr. Robert Traub. We thank Drs. N. Kopell, G.B. Ermentrout, S.B. Colling, C.M. Gray, A. Thomson, N. Tamamaki, T. Freund H. Monyer, and A. Bibbig for helpful discussions, and Drs. R. Walkup and J. Jann for advice with the parallel computers. This work was supported by the Wellcome Trust, the Medical Research Council, IBM, and the Human Frontier Science Program. Slice experiments were performed at Imperial College and the University of Birmingham, and computer simulations at the IBM T.J. Watson Research Center.

1. Singer, W. & Gray, C. M. (1995) *Annu. Rev. Neurosci.* **18,** 555–556.
2. Eckhorn, R., Bauer, R., Jordan, W., Brosch, M., Kruse, W., Munk, M. & Reitboeck, H. J. (1988) *Biol. Cybern.* **60,** 121–130.
3. Eeckman, F. H. & Freeman, W. J. (1990) *Brain Res.* **528,** 238–244.
4. Gray, C. M., König, P., Engel, A. K. & Singer, W. (1989) *Nature (London)* **338,** 334–337.
5. Murthy, V. N. & Fetz, E. E. (1992) *Proc. Natl. Acad. Sci. USA* **89,** 5670–5674.
6. Engel, A. K., König, P., Kreiter, A. K. & Singer, W. (1991) *Science* **252,** 1177–1179.
7. Ribary, U., Ionnades, A. A., Singh, K. D., Hasson, R., Bolton, J. P. J., Lado, F., Mogilner, A. & Llinas, R. (1991) *Proc. Natl. Acad. Sci. USA* **88,** 11037–11041.
8. Cobb, S. R., Halasy, K., Vida, I., Buhl, E. H. & Somogyi, P. (1996) *J. Physiol. (London)* **495,** 62P (abstr.).
9. Whittington, M. A., Traub, R. D. & Jefferys, J. G. R. (1995) *Nature (London)* **373,** 612–615.
10. Thomson, A. M. & Radpour, S. (1991) *Eur. J. Neurosci.* **3,** 587–601.
11. Bliss, T. V. P. & Collingridge, G. L. (1993) *Nature (London)* **361,** 31–34.
12. Hebb, D. O. (1949) *The Organization of Behavior* (Wiley, New York).
13. Frien, A., Eckhorn, R., Bauer, R., Woelbern, T. & Kehr, H. (1994) *NeuroReport* **5,** 2273–2277.
14. Traub, R. D., Whittington, M. A., Colling, S. B., Buzsáki, G. & Jefferys, J. G. R. (1996) *J. Physiol. (London)* **493,** 471–484.
15. Whittington, M. A., Stanford, I. M., Colling, S. B., Jefferys, J. G. R. & Traub, R. D. (1997) *J. Physiol. (London)* **502,** 591–607.
16. Traub, R. D., Whittington, M. A., Stanford, I. M. & Jefferys, J. G. R. (1996) *Nature (London)* **383,** 621–624.
17. Deuchars, J. & Thomson, A. M. (1996) *Neuroscience* **74,** 1009–1018.
18. Womble, M. D. & Moises, H. C. (1994) *Synapse* **17,** 69–75.
19. Pantev, C. (1995) *Brain Topogr.* **7,** 321–330.
20. Roelfsema, P. R., Engel, A. K., König, P. & Singer, W. (1997) *Nature (London)* **385,** 157–161.
21. Magee, J. C. & Johnston, J. (1997) *Science* **275,** 209–213.
22. Markram, H., Lübke, J., Frotscher, M. & Sakmann, B. (1997) *Science* **275,** 213–215.
23. Jefferys, J. G. R. (1979) *J. Physiol. (London)* **289,** 35–88.
24. Spruston, N., Schiller, Y., Stuart, G. & Sakmann, B. (1995) *Science* **268,** 297–300.
25. Traub, R. D., Jefferys, J. G. R., Miles, R., Whittington, M. A. & Tóth, K. (1994) *J. Physiol. (London)* **481,** 79–95.
26. Tsubokawa, H. & Ross, W. N. (1996) *J. Neurophysiol.* **76,** 2896–2906.
27. Freeman, W. J. (1979) *Biol. Cybern.* **35,** 21–37.
28. Lynch, G., Muller, D., Seubert, P. & Larson, J. S. O. (1988) *Brain Res. Bull.* **21,** 363–372.